Tailoring Wettability Change on Aligned and Patterned Carbon Nanotube Films for Selective Assembly

Pinghui Li,[†,||] Xiaodai Lim,[†,||] Yanwu Zhu,[†,‡] Ting Yu,[§] Chong-Kim Ong,[†] Zexiang Shen,[§] Andrew Thye-Shen Wee,[†,‡] and Chorng-Haur Sow*[,†,‡]

Department of Physics, National University of Singapore, 2 Science Drive 3, Singapore 117542, National University of Singapore Nanoscience & Nanotechnology Initiative, Singapore, and School of Physical & Mathematical Sciences, Nanyang Technological University, 1 Nanyang Walk, Singapore 637616

Received: October 16, 2006; In Final Form: December 14, 2006

The effects of oxygen reactive ion etching (RIE) on the surface wettability of aligned carbon nanotube (CNT) films have been systematically investigated. It was found that 3 s of RIE treatment could change the surface of CNT films from hydrophobic to more hydrophilic. The degree of modification in the surface wettability of the film could be controlled by the flow rate of O_2 gas during the RIE process. It is proposed that such a surface hydrophobicity change is related to the opened structure and functionalized tip of as-treated CNTs by oxygen reactive ions. More importantly, after the RIE treatment, focused laser pruning was utilized to trim the surface layer of treated CNTs and revert them back to a hydrophobic surface. Combined with the laser pruning technique and O_2 RIE treatment, CNT templates with interlaced wettability surfaces in a stripe pattern have been fabricated. It has been demonstrated that this interlaced and structured wettability pattern can be used to selectively assemble microspheres or quantum dots on the aligned CNT films with desired patterns.

Downloaded via UNIV SCIENCE AND TECHNOLOGY CHINA on January 12, 2021 at 14:47:45 (UTC).
See https://pubs.acs.org/sharingguidelines for options on how to legitimately share published articles.

Introduction

Carbon nanotubes (CNTs) have attracted great interest due to their outstanding mechanical and electrical properties.[1−4] For industrial applications, good control is often demanded over the building and organization of CNT-based architectures to implement various functions. In this regard, it is useful to fabricate aligned arrays of CNTs. To fabricate such samples, plasma enhanced chemical vapor deposition (PECVD) is one of the most popular methods adopted.[5,6] In the development of CNT-based architectures en route to functional hybrid materials,[7−11] selective assembly of various materials onto CNT platforms is highly desirable. Various site-selective chemical functionalizations of non-aligned CNTs by selectively modifying the nanotube tips, inner walls, and outer walls have been investigated.[12,13] However, precise control of the microscale wettability and selective assembly of other materials on aligned CNTs remain great challenges. One of the main hindrances is the super-hydrophobicity of the aligned films with water contact angle higher than 150°,[14,15] restricting their functionalization with materials dispersed in hydrophilic solvent (e.g., water, alcohol). Recently, Jiang et al. reported the adjustment of surface wettability of the aligned CNT films by varying the anisotropic structure of surface.[16] In this technique, the local wettability relies on the orientation of nanotube arrays. Another challenge is the influence of capillary forces during the evaporation process of liquids from CNT films, which would destroy the aligned structure of nanotubes. For example, Ajayan and Kane et al. reported the formation of two-dimensional cellular patterns by the evaporation of water from O_2 plasma-modified aligned CNT films.[17]

In this report, systematic studies of the effect of O_2 reactive ion etching (RIE) on the surface-wettability of aligned multi-walled carbon nanotube (MWNT) films have been conducted. It is found that O_2 RIE can be used to adjust the surface wettability of aligned MWNTs in a rapid and controllable way. By increasing the O_2 flow rate during etching, the surface wettability of aligned MWNTs can be modified from superhydrophobic to hydrophobic and finally hydrophilic with a controllable decrease in contact angles. This modification process is fast and involves only a few seconds of exposure to the O_2 plasma. Using the laser pruning technique,[18] the top layer of a modified MWNTs film can be trimmed away, and the resultant surface reverts back to a more hydrophobic one. Extending the technique further, MWNT templates with interlaced hydrophobic−hydrophilic stripe patterns have been fabricated. By drying different drops of solutions from aqueous suspensions of silica micro-beads, fluorescent microspheres, or CdTe quantum dots (QDs) on these patterned surfaces, we are able to assemble the particles preferentially onto the less hydrophobic CNT stripes. To prevent the collapse of the aligned structures during the drying process,[17,19] the evaporation of the drop of solution is accelerated by carrying out the evaporation process on a heated hotplate at 60 °C. In this way, the aligned structure of CNT films is preserved during the rapid evaporation process. Our results highlight the feasibility of nondestructive selective assembly of functional materials on specific regions of aligned CNTs.

Experimental Methods

Aligned MWNTs were grown on silicon substrates via PECVD.[20] After that, as-grown CNTs were placed inside the chamber of a SAMCO RIE-10N Reactive Ion Etching Unit and

* Corresponding author. Phone: (65) 65162957. Fax: (65) 67776126. E-mail: physowch@nus.edu.sg.
[†] National University of Singapore.
[‡] National University of Singapore Nanoscience & Nanotechnology Initiative.
[§] Nanyang Technological University.
[||] These authors contributed equally to this work.

10.1021/jp066781t CCC: $37.00 © 2007 American Chemical Society
Published on Web 02/01/2007

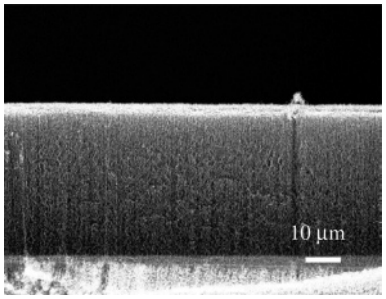

Figure 1. Side-view SEM image of an as-grown CNT film.

pumped down to a base pressure of 4×10^{-6} Torr. O_2 gas was utilized during the treatment. A radio frequency (RF) glow discharge was used to generate the reactive O_2 plasma. CNTs were placed on a RF-driven capacitatively coupled electrode. RF power was set at 20 W, and reflected power was about 1 W. Work pressure was about 0.05 Torr in the chamber, and the temperature was kept at 20 °C. During the RIE process, the flow rate of oxygen was set at 17.25, 24.15, and 34.50 sccm (standard cubic centimeter per minute) with fixed durations of 3, 6, 9, and 12 s. After O_2 RIE treatment, distilled water droplets were then sprinkled onto CNTs surface. Images of droplets were captured using a charge-coupled device (CCD) camera connected to TV-Tuner, which was in turn linked to a laptop for video and image capturing. Manual measurements of contact angles were obtained over an average of around 20 droplet images per sample. The size of water droplets ranged from 60 to 200 μm (calibrated using tungsten wire of diameter 80 μm). During the measurement of O_2 RIE treated CNTs, small volumes of water were sprayed onto the CNT surfaces to avoid the formation of crack patterns. Further characterization of CNTs was carried out using scanning electron microscopy (SEM, JEOL JSM-6400F), transmission electron microscopy (TEM, JEOL JEM-2010F), micro-Raman spectroscopy (Jobin Yvon T64000 system; Ar ion laser with wavelength of 514.5 nm), and X-ray photoelectron spectroscopy (XPS, VG ESCALAB MKII; Mg Kα source). An aqueous suspension of silica micro-beads was diluted from a commercially purchased suspension of silica micro-beads in water with a mean diameter of about 0.71 ± 0.04 μm. 2% aqueous suspensions of red or yellow-green CdTe QDs (Molecular Probes F8786) 20 nm in diameter were commercially purchased from Molecular Probes.

Results and Discussion

The side-view SEM image of an as-grown CNT film is shown in Figure 1. After the aligned nanotube arrays were treated with O_2 RIE, their surface wetting properties were investigated by means of contact angle measurements. As shown in Figure 2, the as-grown aligned CNT film surface is superhydrophobic with a measured contact angle as high as 150.0 ± 5.0°. The variation of the flow rate of O_2 gas during RIE treatment with short etching duration was found to modify the wettability of the sample. By increasing the flow rate of O_2 gas from 17.25 to 24.15 and finally to 34.50 sccm, the water droplet spreads out on the CNT surface gradually with the decrease of contact angle in a controlled manner to 119.4 ± 5.0°, 90.0 ± 5.0°, and 55.0 ± 5.0°, respectively. Such a large decrease of contact angle can be obtained within just 3 s of etching time. Meanwhile, the relationship between the contact angles and the etching time at a fixed O_2 flow rate was also investigated. Figure 2 shows that extending the duration of the etching time beyond 3 s does not have a significant influence on the measured contact angles. For the etching time in the range of 3−12 s, the contact angles are found to remain approximately the same and fluctuate within a small range of ±7.0° under a fixed O_2 flow rate. Thus, the surface wettability change of CNTs mainly occurs in the first 3 s during the RIE treatment.

Further analyses were carried out on the as-grown nanotubes and those treated with 15 s RIE treatment with an O_2 flow rate of 34.5 sccm. First, the diameter of selected individual nanotube

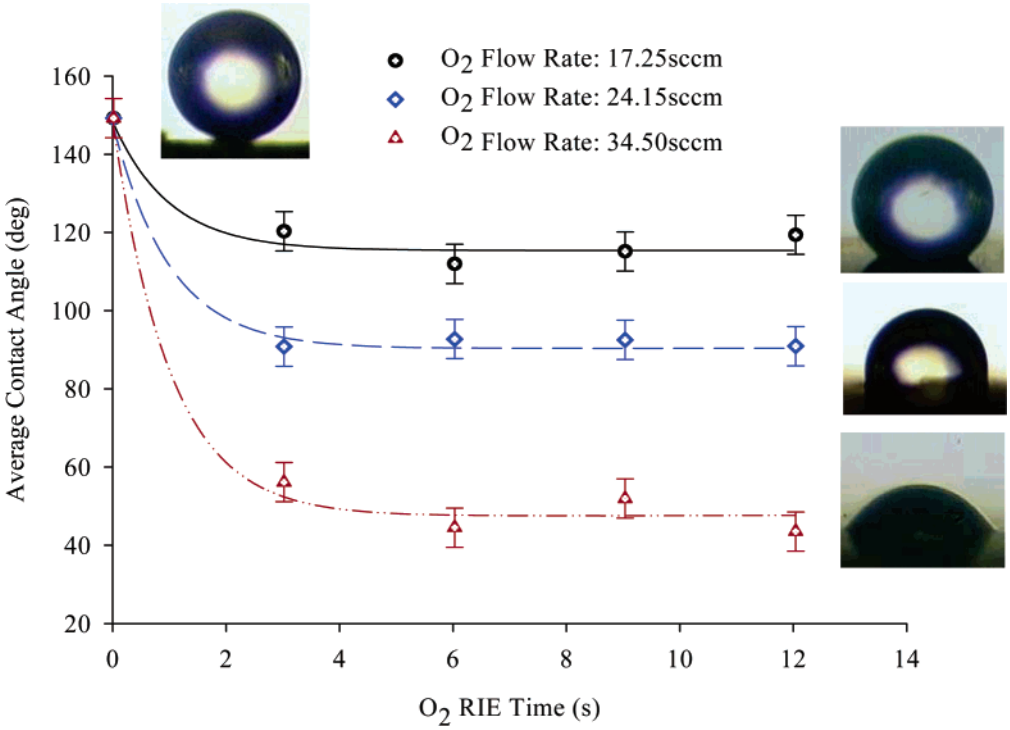

Figure 2. Graph of the variation of contact angles with the change of the O_2 flow rate and RIE time. Contact angle images of the as-grown and RIE treated CNTs are given on the right side of the curves corresponding to the O_2 flow rate of 17.25, 24.15, and 34.5 sccm, respectively.

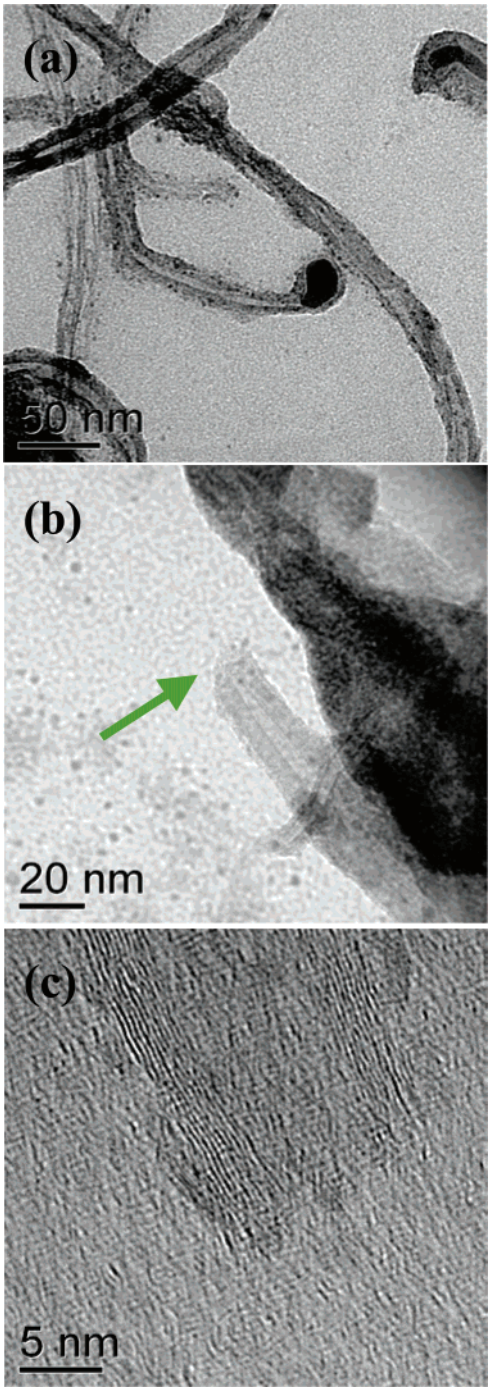

Figure 3. (a) As-grown CNTs with close-ended structure. (b) An open-ended CNT after O_2 RIE treatment. (c) HRTEM image of an open-ended CNT.

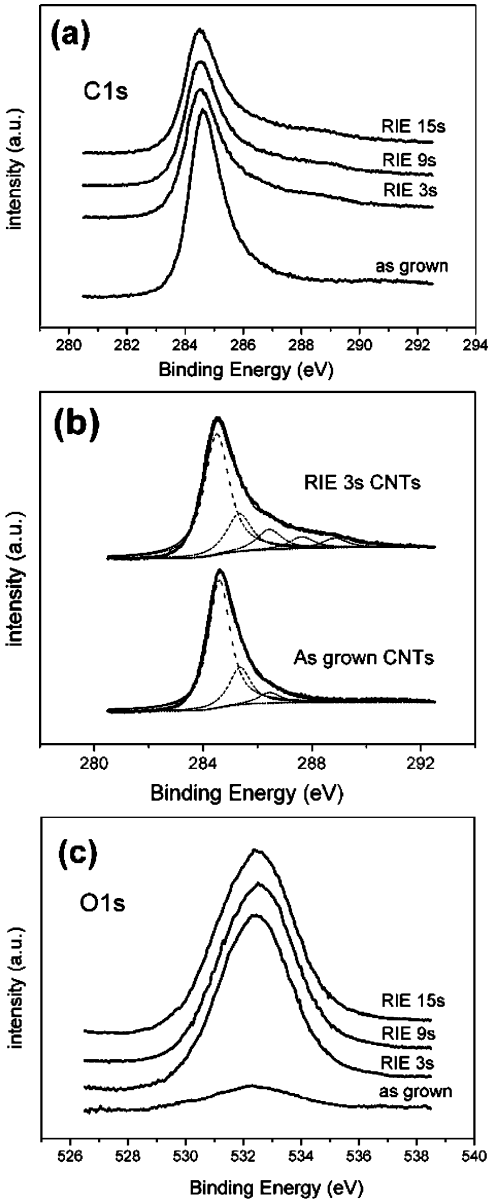

Figure 4. (a) XPS C 1s spectra from as-grown and O_2 RIE treated CNTs. (b) Gaussian decomposition of C 1s spectra of as-grown CNTs and RIE 3 s treated CNTs. (c) O 1s spectra of as-grown and O_2 RIE treated CNTs.

was investigated before and after O_2 RIE treatment. To ensure that the same nanotube was imaged before and after the RIE treatment, a channel made by laser pruning on the as-grown CNT films helps to locate CNT individually (not shown here), similar to our previous reported approach.[21] On the basis of the SEM images, we did not find any significant changes in the diameters of the selected CNTs before and after O_2 RIE treatment, which may be attributed to the short etching time and the rather unreactive CNT sidewalls.

Further studies of the effect of O_2 plasma etching on the MWNT structures were carried out using high-resolution TEM (HRTEM). Figure 3a shows a TEM image of as-grown CNTs, from which we can see that Fe particle is enclosed within the graphite layers. After 15 s RIE treatment with an O_2 flow rate of 34.5 sccm, it is found that some CNTs have open-ended structures. Such results have also been observed in CNTs treated with other plasmas.[22−24] A typical image can be seen from Figure 3b. The ratio of open-ended to close-ended CNTs is about 1:1 based on the random selection during the TEM observations. Figure 3c shows a HRTEM image of an open-ended CNT with 10 graphite layers. Some graphite layers of cylindrical walls near the tips are broken due to the plasma etching, similar to a previous report of O_2 plasma-oxidized CNTs but with fewer defects due to the short etching time.[25] After RIE treatment, it is possible that open-ended CNT structures are created in our sample. There is a likelihood that internal wetting occurs in some of the CNTs, especially those with smaller internal diameter.[26−28] Such a possible effect may affect the whole surface wettability and thus the contact angle of the sample.

XPS measurements were carried out to investigate the chemical states on the surface of the as-grown and RIE treated

CNTs. Here, the flow rate of O_2 during the RIE period was 34.5 sccm. Figure 4a shows that the C 1s peak intensity is reduced and a high binding energy shoulder appears after the O_2 RIE treatment, which implies the formation of strong C and O bonds. The Gaussian decomposition of the peaks of as-grown and RIE 3 s treated CNTs is shown in Figure 4b. For the as-grown CNTs, the spectrum consists of at least three peaks. The peaks at about 284.6, 285.3, and 286.5 eV are attributed to the graphite sp^2 component, diamond-like sp^3 component, and C−OH group or C═O bond of the aromatic group, respectively. [29−32] For RIE 3 s treated CNTs, the spectrum can be decomposed into five peaks. The additional two peaks at about 287.6 and 288.8 eV are assigned to C═O of the aliphatic group and OH−C═O group, respectively.[29] It is generally accepted that, for CNTs, the carboxyl groups are mainly situated on the open ends of the tubes and the edges of the sheets, whereas the hydroxyl and carbonyl groups are more likely to be found on the basal planes and tube walls, respectively.[29] The observation of OH−C═O group for the O_2 RIE treated open-ended CNTs is consistent with this claim. Comparing the C 1s curves representing RIE 3, 9, and 15 s treated CNTs, we observe almost no difference in shape from the graphs. Correspondingly, the Gaussian decomposition of the peaks of RIE 9 or 15 s treated CNTs is similar to the RIE 3 s treated one. All of these indicate that the chemical bonds are mainly formed in the first 3 s, which is consistent with the nearly stable contact angles after 3 s shown in Figure 2. Figure 4c shows the increase in the intensity of O 1s spectra after O_2 RIE treatment. Again, the variation of etching time from 3 to 15 s does not increase the oxygen concentration of CNTs obviously using the O_2 flow rate of 34.5 sccm. Based on the XPS study, it is found that some hydrophilic chemical bonds such as OH−C═O have been formed at the open-ends of CNTs, indicating an important factor contributing to the fast wettability change after the O_2 RIE treatment.

Raman spectra of as-grown and O_2-RIE treated CNTs were shown in Figure 5a to further investigate the structure change. All spectra show mainly two peaks at about 1353 cm^{-1} (D band) and 1595 cm^{-1} (G band), which correspond to amorphous and graphite carbon signals, respectively.[33,34] Figure 5b shows the dependence of the ratio of D-band to G-band intensity (I_D/I_G) on RIE time. The ratio of I_D/I_G decreases significantly for the 3 s RIE treated sample, and then increases gradually with further increasing the RIE time. Previous studies showed that the tips of aligned CNTs are more reactive and easily removed by plasma.[23,24] At the same time, the top-layer of CNTs contains more disordered or amorphous carbon than the lower portion. The removal of the amorphous portion could contribute to the observed decrease of I_D/I_G ratio. Further etching will destroy the cylindrical walls of the CNTs near the tips. As a result, the ratio of I_D/I_G increases slightly with longer etching time.

During the RIE treatment of a dense film of aligned CNTs array, it is reasonable to believe that the upper portion of the CNTs facing the plasma would shield the lower portion from etching. Thus, the modification of the CNTs is primarily on the surface of the sample. In other words, if the top layer of the CNTs films is carefully trimmed away, the resultant aligned CNTs film could revert to a hydrophobic one. To carry out this investigation, we made use of the laser pruning technique,[18] to trim away the top layer of a treated CNTs film, and we studied its wettability. Experimental details are given as follows: First, an as-grown CNT film was treated by O_2 RIE etching for 15 s with an O_2 flow rate of 24.15 sccm. After that, half of the area of the CNT film was exposed to a scanning focused laser

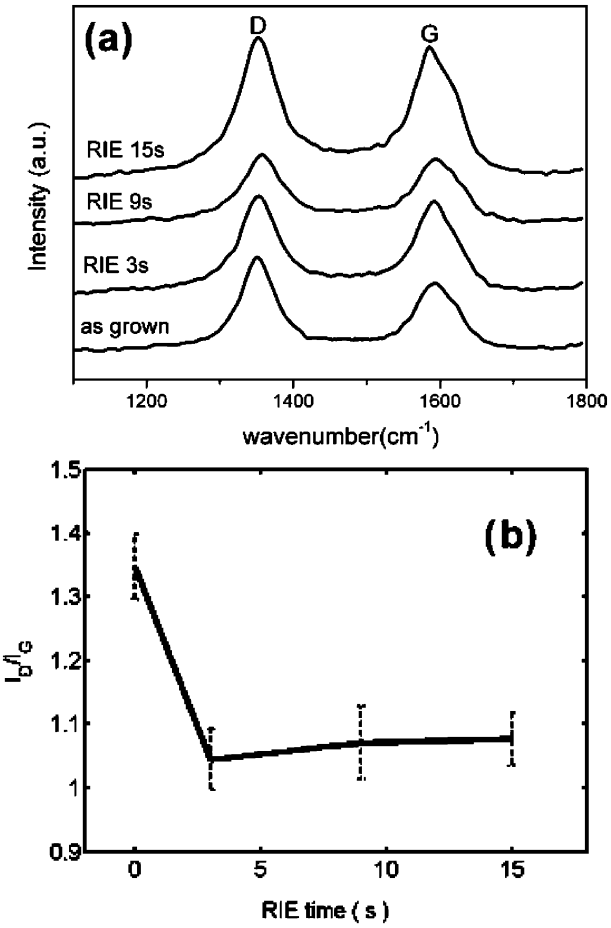

Figure 5. (a) Micro Raman spectra of as-grown and O_2 RIE 3, 9, and 15 s treated CNTs with the flow rate of 34.5 sccm. (b) Plot of the ratio of D-band over G-band intensity (I_D/I_G) as a function of RIE time.

beam that trimmed away the upper portion of the CNTs.[18] The side-view SEM image in Figure 6a shows O_2 pretreated CNTs and laser-trimmed CNTs. The lengths of the O_2 pretreated CNTs are about 40 μm with a surface contact angle of about 96.0 ± 5.0°, as shown in Figure 6c. By adjusting the laser beam power of the focused laser beam, we can selectively trim only the upper portion of some of the aligned CNTs array. The length of the remained CNTs in the laser-trimmed regions is about 25 μm, as seen in Figure 6b. The surface contact angle measurements show that these laser-trimmed CNTs have a contact angle of about 126.0 ± 5.0°. Thus, with laser trimming, the CNTs films revert to a more hydrophobic film. Jiang et al. reported that a large amount of air trapping is important for the super-hydrophobicity of aligned-structure films.[35−39] The increase in the fraction of trapped air on the surface would result in a larger contact angle according to Cassie's law.[40] Top-view SEM images of the laser-trimmed and untrimmed CNTs with the same magnification are given in Figure 6d and e, respectively. As can be seen in these figures, the density of CNTs in the laser-trimmed part is much lower than that of the untrimmed part. Such a lower density of CNTs would produce a larger amount of air trapping and correspondingly result in a bigger contact angle. Meanwhile, it was reported that the lengths of CNTs do not affect the measured contact angles greatly for the study of PECVD grown aligned carbon nanotube films.[15] Thus, the recovery of the hydrophobicity in the trimmed

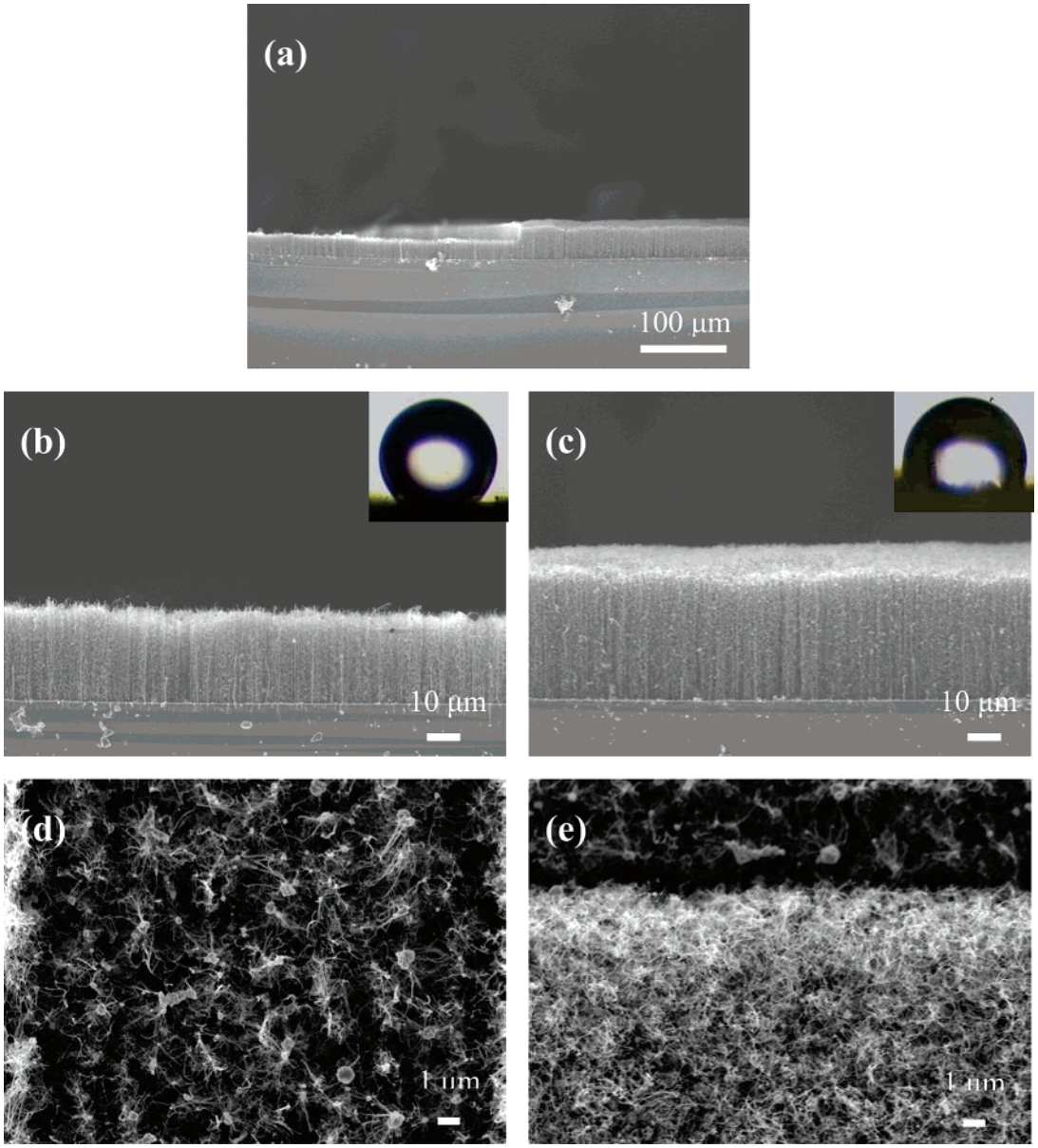

Figure 6. (a) Typical SEM image of laser-half-trimmed CNT film pretreated by O_2 RIE etching. (b) Side-view image of laser-trimmed CNTs with a surface contact angle of about 126.0 ± 5.0°. (c) Side-view image of the laser-untrimmed part with a surface contact angle of about 96.0 ± 5.0°. (d) SEM image of laser-trimmed CNTs. (e) Untrimmed CNTs.

CNTs is attributed to the removal or reduction of effects brought about by O_2 RIE and the increase of air trapping among CNTs.

Using the focused laser pruning technique, it is straightforward to create a wide variety of patterns comprised of interlaced hydrophobic and hydrophilic regions. A direct application from this is to fabricate CNT templates with microscale controllable surface wettability for selective assembly of nanoparticles suspended in aqueous suspension. Figure 7a shows the SEM image of a periodic array of CNT grooved patterns in stripe formation. The width of the grooves is about 10 μm. Because the pattern was created from a CNT film treated with 15 s of RIE etching with an O_2 flow rate of 24.15 sccm, the laser-trimmed grooves are more hydrophobic in nature. A close-up view of the pattern created is shown in the inset. Particle assembly behavior on these CNT films with interlaced wettability was investigated. To avoid the formation of the cellular patterns during the evaporation process,[17] the CNT films were placed on a hotplate at a temperature of 60 °C to accelerate the evaporation process of the solution. Next, a drop of colloidal solution comprising an aqueous suspension of silica micro-beads in water with the diameter of 0.71 ± 0.04 μm was placed on the film surface. The drying process lasted for several seconds. By taking SEM images of the same regions, it is found that the silica micro-beads selectively assemble on the hydrophilic regions (i.e., regions not trimmed by the laser beam). A large-scale image is shown in Figure 7b. No silica micro-beads were observed in the laser-trimmed grooves. From the side-view in Figure 7c, it can be seen that all of the micro-beads are assembled on the top surface of the CNT stripes, while the lower portion of the CNTs retains the aligned structure. By using the same method, a "NUS" pattern decorated with silica micro-beads is obtained, as shown in Figure 7d.

To further test the versatility of the selective assembly of the patterned CNT template with interlaced wettability, 20 nm fluorescent microspheres or glutathione capped CdTe QDs dispersed in water solution were used in separate experiments.[41] The photoluminescence (PL) peak of the CdTe QDs is around

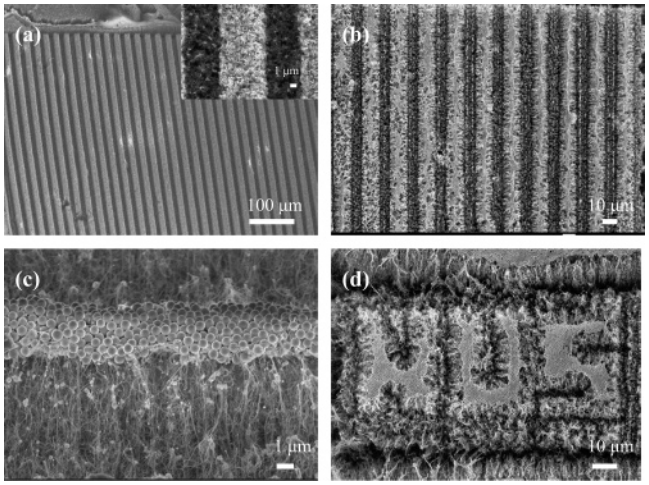

Figure 7. (a) CNT grooves produced on O_2 RIE pretreated aligned CNT film. Inset is a close view of the CNT grooves. (b) Selective assembly of silica micro-beads on the laser-untrimmed CNT stripes with typical side-view images given in (c). (d) "NUS" pattern decorated with silica micro-beads.

570 nm. By using the same hotplate heating methods, we have successfully assembled fluorescent microspheres and glutathione capped CdTe QDs preferentially onto the pre-patterned hydrophilic regions of the CNT templates. Figure 8a shows the fluorescent image of the hydrophilic CNT stripes with fluorescent microspheres on their surface. No red light has been observed from the hydrophobic regions because they do not contain any fluorescent microspheres. A close-up view can be seen from Figure 8b. Figure 8c and d shows the bright-field optical microscopy images of the CNT template decorated with CdTe QDs by focusing on the lower more hydrophobic CNT groove regions and the higher less hydrophobic regions, respectively. The observed red/orange light was emitted from the regions decorated with CdTe QDs on their surface, which indicates that the CdTe QDs assembled selectively onto the less hydrophobic regions of the CNT template.

Additional experiments were conducted to investigate if efficient selective assembly can be achieved using CNT surfaces with contrasting wettability but not structural features as defined by focused laser beam. In these experiments, aligned MWNT films covered with copper grids with honeycomb patterns (commonly used as sample holder for TEM imaging, Figure 9a) were exposed to RIE as before. Regions of the surface protected by the grid remained hydrophobic, while the exposed region became converted to hydrophilic ones. A drop of colloidal solution comprising an aqueous suspension of 20 nm yellow-green fluorescent microspheres was then placed on the surface of the samples. Figure 9b shows the fluorescent image of selective assembly of fluorescent microspheres on the modified MWNT film. It is evident that the fluorescent microspheres preferentially assembled onto the hydrophilic part of the sample. However, the boundary between the hydrophilic and hydrophobic part is not as well defined as before. Thus, a dual combinatory approach of wettability modification and structural architecture proved to be more desirable in directed assembly of these nanoparticles.

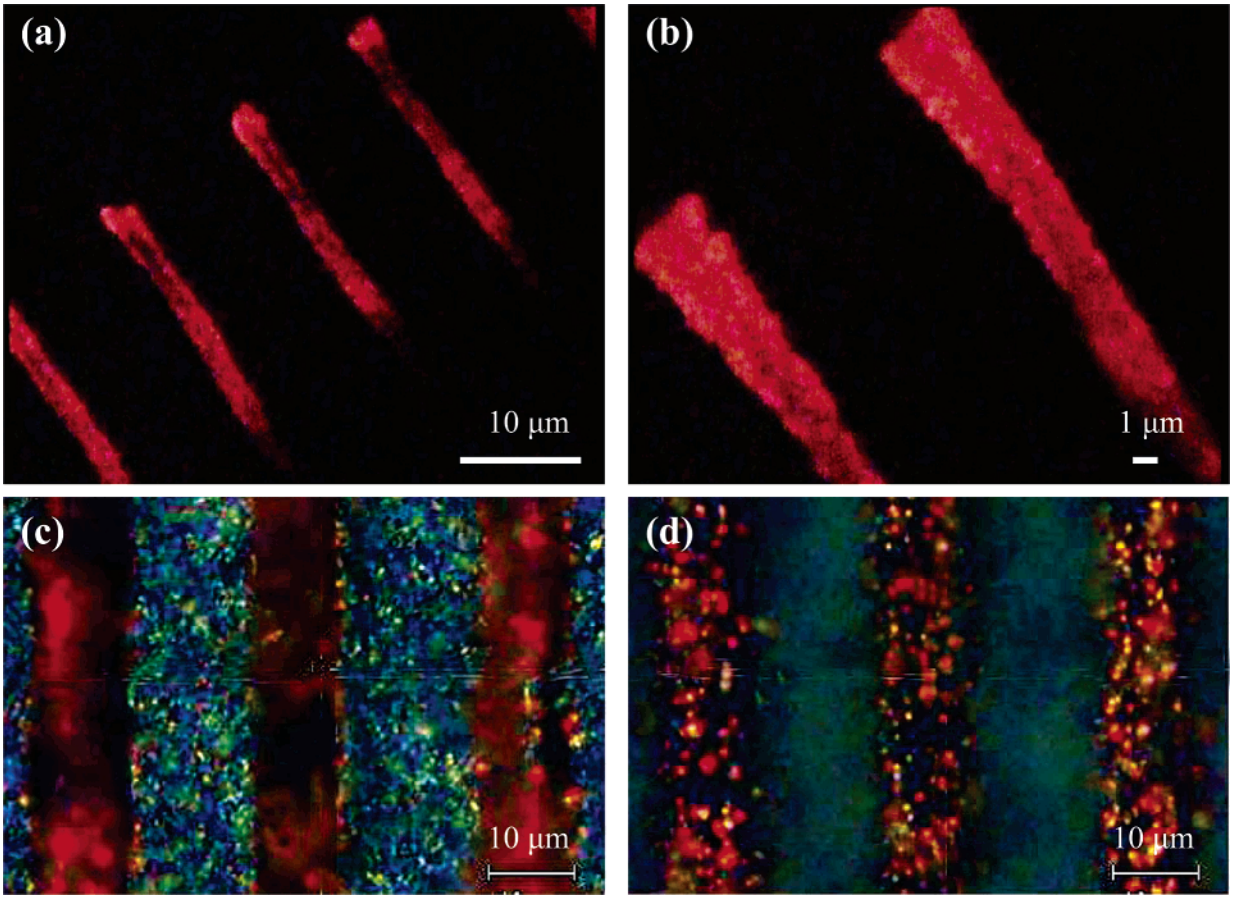

Figure 8. (a) Selective assembly of fluorescent microspheres on the laser-untrimmed CNT stripes examined by the fluorescence microscopy. (b) A close view of the fluorescent microspheres decorated CNT stripes. (c) and (d) are the bright-field optical microscopy images of the CNT template decorated with CdTe QDs by focusing on the lower more hydrophobic CNT groove regions and the higher less hydrophobic regions, respectively.

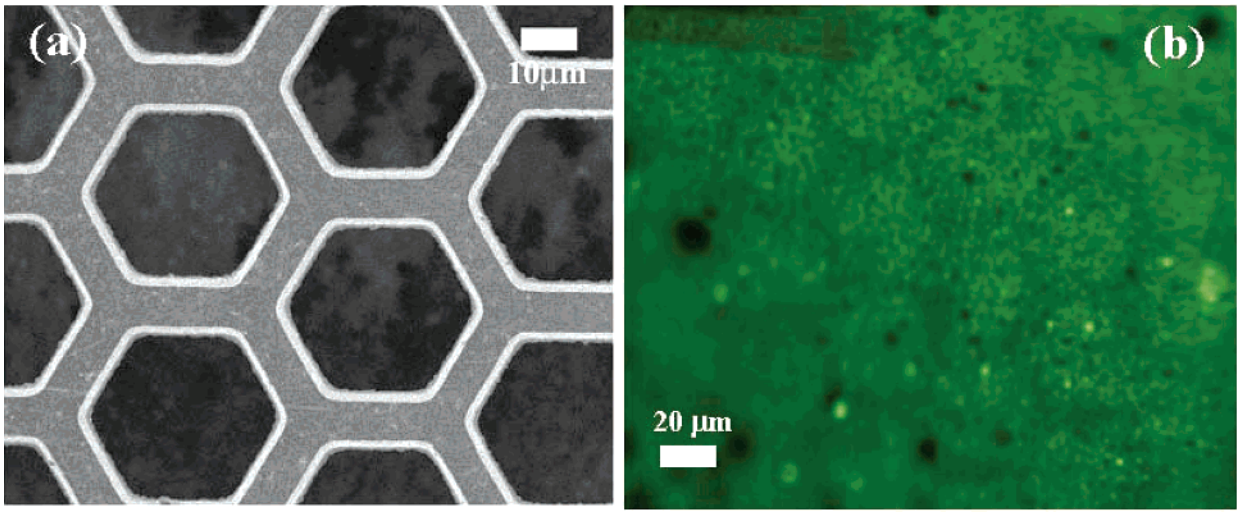

Figure 9. (a) SEM image of copper grids used to cover the MWNT film during the RIE treatment. (b) Fluorescent microscope image of selective assembly of fluorescent microspheres on the modified MWNT film.

Conclusions

In conclusion, controllable and rapid wettability change on the aligned CNT surface induced by O_2 reactive ion etching has been investigated. More importantly, CNT templates with interlaced wettability surfaces in a stripe pattern have been fabricated with the focused laser pruning method. Such aligned CNT templates with controlled microscale-wettability make it possible to selectively assemble materials on the aligned CNT surface with accelerated evaporation. This technique is potentially useful for the fabrication of patterned hybrid−material systems based on aligned CNT films.

Acknowledgment. P. L. thanks L. H. Van, K. C. Chin, K. A. Mahabadi, Z. H. Ni, C. H. Teo, and F. C. Cheong for their assistance in experiments and characterizations. C.-H.S. would like to acknowledge support from ASTAR PMED TSRP Research Grant.

References and Notes

(1) Ebbesen, T. W. *Carbon Nanotubes, Preparation and Properties*; CRC Press: Boca Raton, FL, 1997.
(2) Dresselhaus, M.; Dresselhaus, G.; Eklund, P.; Saito, R. *Phys. World* **1998**, 33.
(3) Javey, A.; Guo, J.; Wang, Q.; Lundstrom, M.; Dai, H. *Nature* **2003**, *424*, 654.
(4) Qi, P.; Javey, A.; Rolandi, M.; Wang, Q.; Yenilmez, E.; Dai, H. *J. Am. Chem. Soc.* **2004**, *126*, 11774.
(5) Ren, Z. F.; Huang, Z. P.; Xu, J. W.; Wang, J. H.; Bush, P.; Siegal, M. P.; Provencio, P. N. *Science* **1998**, *282*, 1105.
(6) Meyyappan, M.; Delzeit, L.; Cassell, A.; Hash, D. *Plasma Sources Sci. Technol.* **2003**, *12*, 205.
(7) Zhu, Y.; Elim, H. I.; Foo, Y. L.; Yu, T.; Liu, Y.; Ji, W.; Lee, J. Y.; Shen, Z.; Wee, A. T. S.; Thong, J. T. L.; Sow, C. H. *Adv. Mater.* **2006**, *18*, 157.
(8) Chin, K. C.; Gohel, A.; Chen, W. Z.; Elim, H. I.; Ji, W.; Chong, G. L.; Sow, C. H.; Wee, A. T. S. *Chem. Phys. Lett.* **2005**, *409*, 85.
(9) de Heer, W. A.; Poncharal, P.; Berger, C.; Gezo, J.; Song, Z.; Bettini, J.; Ugarte, D. *Science* **2005**, *307*, 907.
(10) Ye, J. S.; Cui, H. F.; Liu, X.; Lim, T. M.; Zhang, W. D.; Sheu, F. S. *Small* **2005**, *1*, 560.
(11) Osterloh, F. E.; Martino, J. S.; Hiramatsu, H.; Hewitt, D. P. *Nano Lett.* **2003**, *3*, 125.
(12) Hirsch, A. *Angew. Chem., Int. Ed.* **2002**, *41*, 1853.
(13) Bahr, J. L.; Tour, J. M. *J. Mater. Chem.* **2002**, *12*, 1952.
(14) Li, H.; Wang, X.; Song, Y.; Liu, Y.; Li, Q.; Jiang, L.; Zhu, D. *Angew. Chem., Int. Ed.* **2001**, *40*, 1743.
(15) Lau, K. K. S.; Bico, J.; Teo, K. B. K.; Chhowalla, M.; Amaratunga, G. A. J.; Milne, W. I.; McKinley, G. H.; Gleason, K. K. *Nano Lett.* **2003**, *3*, 1701.
(16) Sun, T.; Wang, G.; Liu, H.; Feng, L.; Jiang, L.; Zhu, D. *J. Am. Chem. Soc.* **2003**, *125*, 14996.
(17) Chakrapani, N.; Wei, B.; Carrillo, A.; Ajayan, P. M.; Kane, R. S. *Proc. Natl. Acad. Sci. U.S.A.* **2004**, *101*, 4009.
(18) Lim, K. Y.; Sow, C. H.; Lin, J. Y.; Cheong, F. C.; Shen, Z. X.; Thong, J. T. L.; Chin, K. C.; Wee, A. T. S. *Adv. Mater.* **2003**, *15*, 300.
(19) Liu, H.; Li, S.; Zhai, J.; Li, H.; Zheng, Q.; Jiang, L.; Zhu, D. *Angew. Chem., Int. Ed.* **2004**, *43*, 1146.
(20) Wang, Y. H.; Lin, J.; Huan, C. H. A.; Chen, G. S. *Appl. Phys. Lett.* **2001**, *79*, 680.
(21) Zhu, Y. W.; Moo, A. M.; Yu, T.; Xu, X. J.; Gao, X. Y.; Liu, Y. J.; Lim, C. T.; Shen, Z. X.; Ong, C. K.; Wee, A. T. S.; Thong, J. T. L.; Sow, C. H. *Chem. Phys. Lett.* **2006**, *419*, 485.
(22) Zhi, C. Y.; Bai, X. D.; Wang, E. G. *Appl. Phys. Lett.* **2002**, *81*, 1690.
(23) Zhu, Y. W.; Cheong, F. C.; Yu, T.; Xu, X. J.; Lim, C. T.; Thong, J. T. L.; Shen, Z. X.; Ong, C. K.; Liu, Y. J.; Wee, A. T. S.; Sow, C. H. *Carbon* **2005**, *43*, 395.
(24) Huang, S.; Dai, L. *J. Phys. Chem. B* **2002**, *106*, 3543.
(25) Ago, H.; Kugler, T.; Cacialli, F.; Salaneck, W. R.; Shaffer, M. S. P.; Windle, A. H.; Friend, R. H. *J. Phys. Chem. B* **1999**, *103*, 8116.
(26) Rossi, M. P.; Ye, H.; Gogotsi, Y.; Babu, S.; Ndungu, P.; Bradley, J. C. *Nano Lett.* **2004**, *4*, 989.
(27) Kim, B. M.; Sinha, S.; Bau, H. H. *Nano Lett.* **2004**, *4*, 2203.
(28) Barber, A. H.; Cohen, S. R.; Wagner, H. D. *Phys. Rev. B* **2005**, *71*, 115443.
(29) Kovtyukhova, N. I.; Mallouk, T. E.; Pan, L.; Dickey, E. C. *J. Am. Chem. Soc.* **2003**, *125*, 9761.
(30) Felten, A.; Bittencourt, C.; Pireaux, J. J.; Van Lier, G.; Charlier, J. C. *J. Appl. Phys.* **2005**, *98*, 074308.
(31) Liu, M.; Yang, Y.; Zhu, T.; Liu, Z. *Carbon* **2005**, *43*, 1470.
(32) Shan, Y.; Gao, L. *Nanotechnology* **2005**, *16*, 625.
(33) Lee, Y. T.; Kim, N. S.; Bae, S. Y.; Park, J.; Yu, S. C.; Ryu, H.; Lee, H. J. *J. Phys. Chem. B* **2003**, *107*, 12958.
(34) Kayastha, V.; Yap, Y. K.; Dimovski, S.; Gogotsi, Y. *Appl. Phys. Lett.* **2004**, *85*, 3265.
(35) Li, S.; Li, H.; Wang, X.; Song, Y.; Liu, Y.; Jiang, L.; Zhu, D. *J. Phys. Chem. B* **2002**, *106*, 9274.
(36) Liu, H.; Li, S.; Zhai, J.; Li, H.; Zheng, Q.; Jiang, L.; Zhu, D. *Angew. Chem., Int. Ed.* **2004**, *43*, 1146.
(37) Feng, L.; Li, S.; Li, Y.; Li, H.; Zhang, L.; Zhai, J.; Song, Y.; Liu, B.; Jiang, L.; Zhu, D. *Adv. Mater.* **2002**, *14*, 1857.
(38) Feng, L.; Song, Y.; Zhai, J.; Liu, B.; Xu, J.; Jiang, L.; Zhu, D. *Angew. Chem., Int. Ed.* **2003**, *42*, 800.
(39) Jin, M.; Feng, X.; Feng, L.; Sun, T.; Zhai, J.; Li, T.; Jiang, L. *Adv. Mater.* **2005**, *17*, 1857.
(40) Cassie, A. B. D. *Discuss. Faraday Soc.* **1948**, *3*, 11.
(41) Ying, J. Y.; Zheng, Y.; Gao, S. PCT Patent No. 60/666,731.